Microscopic analysis of generation-recombination noise in semiconductors under dc and time-varying electric fields

S. Pérez and T. González[a)]
Departamento de Física Aplicada, Facultad de Ciencias, Universidad de Salamanca, Plaza de la Merced s/n, 37008 Salamanca, Spain

S. L. Delage
THOMSON-CSF/Laboratoire Central de Recherches, Domaine de Corbeville, 91404 Orsay Cédex, France

J. Obregon
IRCOM. CNRS. Université de Limoges, 123, Av. Albert Thomas, 87060 Limoges Cédex, France

(Received 10 March 2000; accepted for publication 18 April 2000)

We present a microscopic analysis of current fluctuations in a semiconductor sample in the presence of trapping–detrapping processes and conventional scattering mechanisms. An ensemble Monte Carlo simulation is used for calculations. To ensure the linearity of the system, we use a model where the characteristic times of the different microscopic mechanisms are considered as energy independent. We analyze the behavior of thermal and generation-recombination noise spectra under static (dc field) and time-varying (ac field) conditions. Under dc bias we confirm the validity of the microscopic model by comparing the results of the simulation with analytical predictions. When an ac field is applied, amplitude modulation of the semiconductor response takes place due to generation-recombination processes. This modulation leads to the upconversion of the low-frequency generation-recombination spectrum, which is evidenced (even in the absence of dc current) and analyzed under different physical conditions. © *2000 American Institute of Physics.* [S0021-8979(00)09114-3]

I. INTRODUCTION

The low-frequency noise of electronic devices is known to be very sensitive to defects introduced during the semiconductor growth process and the different steps of the fabrication technology.[1] In particular, generation-recombination (GR) phenomena associated to these defects are a fundamental source of noise at this frequency range. For example, the fluctuating occupancy of deep level traps in the depletion region and channel is the dominant mechanism for GR noise in field effect transistors.[2]

The knowledge of these processes is essential, since $1/f$ noise in several devices has been attributed to the superposition of individual GR noise spectra produced by a trap distribution in the band gap.[3] Many studies have been carried out to investigate the origin of this kind of noise and to find its mathematical description. Some of them consider this GR noise as resistance fluctuations due to carrier number fluctuations.[4,5]

Moreover, the low-frequency noise behavior of active devices may be of significant importance also at high frequencies, not only in the case of nonlinear circuits sensitive to phase noise, such as oscillators and mixers,[6,7] but also when the amplitude modulation of ac signals occurs. In fact, though $1/f$ noise in resistors is usually measured when a dc current is flowing, some authors assert that an ac method can, under certain circumstances, provide more accurate noise measurements than the dc method does.[8–10] When an ac voltage with frequency f_{ac} is supplied to the resistor, fluctuations due to GR processes will cause amplitude modulation of the ac current response. Therefore, noise measurements will show an alternating response current at the frequency f_{ac} accompanied at both sides of the spectrum by an additional noise contribution that is called $1/\Delta f$ noise. This ac method exhibits a perfect agreement between the calculated and observed ratio of the $1/\Delta f$ noise magnitude with respect to that of $1/f$ noise when measured with dc current.[9]

Among the several techniques suitable for the analysis of electronic noise in semiconductor devices, the Monte Carlo (MC) method has been proved to be especially powerful when a microscopic description of the system under investigation is required.[11] While widely used for the analysis of noise at high frequencies (in the microwave range and beyond) in semiconductor materials and devices,[11–18] very few attempts have been carried out to use this technique when low-frequency processes (as compared with the typical frequencies of scattering mechanisms) take place,[19–22] as is the case of GR phenomena. This is mainly due to the large difference existing between the scattering rates of both types of mechanisms, which leads to very long computation times. The aim of this article is to present a MC study of current fluctuations in semiconductors in the presence of dc as well as time-varying (sinusoidal) applied electric fields (ac fields) when both scattering and GR processes are considered. This microscopic approach allows us to include in the simulation GR processes in the same way as conventional scattering mechanisms described by transition rates between micro-

a)Electronic mail: tomasg@gugu.usal.es

scopic states of carriers. Consequently, the knowledge of phenomenological parameters as the variance of carrier number fluctuations $\langle \Delta N^2 \rangle$ and the carrier lifetime τ_l usually necessary in analytical approaches is not needed. Up to now, in the few published papers where MC simulations include GR noise sources, only a dc voltage is considered.[19–22] However, numerical simulations of the influence of GR noise on the semiconductor response to time-varying signals are needed in order to interpret experimental and theoretical results. Therefore, present findings should provide a substantial improvement in the study of electronic noise in semiconductor materials in the presence of an external ac electric field.

For the calculations we have used an ensemble MC simulator three dimensional in momentum space.[23] A thermalizing energy-independent scattering model[19] ensuring the linearity of the semiconductor response at any bias is used to avoid harmonic generation in the ac response. In addition GR processes associated with electron traps characterized by a single energy level are considered. This model allows us to study the effect of number and thermal fluctuations on the current noise. We perform the analysis of current fluctuations under both dc and ac electric fields. The dc results are a first and very important step in understanding the fluctuations, since they provide information concerning the processes at the origin of the noise behavior. Special attention has been paid to the spectral density of current fluctuations under ac bias for different trapping and detrapping probabilities and ac field magnitude to characterize the upconversion of low-frequency noise to high frequencies that is detected in the results.

The article is organized as follows. In Sec. II the physical system under analysis is described, Sec. III provides the details of the MC simulation, and in Sec. IV the results obtained under both dc and ac bias are reported. Section V summarizes the main conclusions and future trends of our work.

II. PHYSICAL MODEL

We consider an *N*-type homogeneous semiconductor of length L and cross-sectional area A at temperature $T = 300$ K. Free electrons are provided by donor levels close to the bottom of the conduction band, which are completely ionized at the temperature of interest. A single type of electron traps at a depth E_n below the bottom of conduction band is present in the semiconductor. It is assumed that the traps interact only with electrons in the conduction band, in such a way that the electrons provided by the donor impurities are distributed over the conduction band and the traps.

Within this model, free electrons disappear by trapping at the rate $v_{\mathrm{th}} s (N_t - n_t) n$, where v_{th} is the thermal velocity of free carriers, s the capture cross section of the traps, N_t the density of electron traps, n_t the density of trapped electrons, and n the free-carrier density; and trapped electrons are released at the rate $\nu_0 \exp(-eE_n/kT) n_t$, where ν_0 is a vibration frequency and k Boltzmann constant.[24] Therefore, there are two time constants involved in the trapping–detrapping process: the recombination time, τ_r (average ''free time'' of an electron), and the generation time, τ_g (average ''captured time'' of an electron), respectively, given by

$$\frac{1}{\tau_r} = v_{\mathrm{th}} s (N_t - n_t), \tag{1}$$

$$\frac{1}{\tau_g} = \nu_0 \exp\left(- \frac{eE_n}{kT} \right). \tag{2}$$

As long as $n_t \ll N_t$ (as it is assumed in our model), both times can be considered to be independent of the occupancy of the traps.

In order to avoid a nonlinear response of the semiconductor to external electric fields (absence of harmonic generation for ac fields) and thus to detect clearly the influence of GR phenomena, a simple model is used to describe the semiconductor.[19] The conduction band is assumed to be spherical and parabolic, characterized by an effective mass m. In addition to the presence of recombination processes, free electrons move under the action of scattering mechanisms, which are characterized by an energy-independent relaxation time τ_s and are assumed to be isotropic and completely thermalizing. The length of the sample L is assumed to be much longer than the carrier mean free path $l = v_{\mathrm{th}} \tau_s$, so that the noise behavior is the same as that of an infinite sample (bulk semiconductor). Due to the action of inelastic scattering, electrons remain quite close to equilibrium conditions even if an electric field is applied. Consequently, the recombination time τ_r can be considered to be also energy independent.

The above model is implemented by means of an ensemble MC simulation three dimensional in momentum space. An initial number of thermal free carriers N is considered, which move under the action of the applied electric field and the influence of scattering and trapping mechanisms. During the carrier movement there are probabilities per unit time $1/\tau_s$ and $1/\tau_r$ that an electron is scattered or captured, respectively. Accordingly, the free-flight time t_f can be determined stochastically as $t_f = -\tau_f \ln r$, where $\tau_f = \tau_s \tau_r / (\tau_s + \tau_r)$ and r is a random number uniformly distributed between 0 and 1. At the end of the free flight, the type of process taking place, scattering or trapping, is randomly selected according to the respective probabilities. If a scattering process occurs, the carrier is thermalized and, correspondingly, its velocity components are randomly determined according to a Maxwellian distribution at the lattice temperature. If the carrier is captured, it remains trapped (with null velocity) during a time t_t, which is stochastically determined, according to the detrapping probability per unit time $1/\tau_g$, as $t_t = -\tau_g \ln r$. When the carrier is released, its velocity components are also determined according to a Maxwellian distribution at the lattice temperature. As a consequence of these dynamics, at a given time t of the simulation $N_f(t)$ of the initial N carriers will be free in the conduction band and $N_c(t)$ will be captured in the traps, being always $N = N_f(t) + N_c(t)$. During the simulation the quantities of interest (average electron velocity and energy, number of free and trapped carriers, etc.) are recorded at fixed time intervals Δt in order to perform the noise calculations described in next section.

The electric field E is applied to the semiconductor in the x direction. According to the Ramo–Shockley theorem, the short-circuit current flowing through the semiconductor sample under the assumption of constant applied voltage (i.e., constant electric field) is given by[11]

$$I(t)=\frac{q}{L}\sum_{i=1}^{N_f(t)} v_{xi}(t), \tag{3}$$

where q is the electron charge and $v_{xi}(t)$ the instantaneous x velocity of the ith carrier. Notice that $I(t)$ can fluctuate due to both the effect of scattering on $v_{xi}(t)$ (thermal noise) and of GR phenomena on $N_f(t)$ (GR noise). We will first analyze the noise behavior of the sample under a static electric field to evidence the influence of both types of noise. Then we will study the effect of trapping–deterapping processes in the semiconductor response to a time-varying field, leading to the upconversion of the low-frequency GR noise spectrum. In the latter case, a second term proportional to the time derivative of the potential applied to the electrodes would appear in $I(t)$,[11] which would lead to the presence of a peak at the frequency of the ac signal in the current spectrum. We will ignore such a term, since we are only interested in the bulk response of the semiconductor.

For the calculations we have used the following set of parameters: $m=0.25m_0$ (m_0 being the free-electron mass), $N=1000$, $\tau_s=10^{-14}$ s, τ_r ranging from 2×10^{-12} to 10^{-10} s, and τ_g ranging from 2×10^{-12} to 10^{-9} s. In the case of the ac analysis, in order to avoid extremely long simulation times, a frequency $f_{\rm ac}$ of 500 GHz is taken for the electric field. The total simulated time is of the order of 10^{-9}–10^{-8} s in the case of dc fields and 10^{-8}–10^{-7} s for ac fields. Typically, a time interval Δt of 2×10^{-15} s is used to sample the different quantities. Notice that the typical hierarchy of the characteristic times in the simulation is $\tau_s<\tau_{\rm ac}<\tau_r,\tau_g$. Even if some of these times could be found unrealistic (especially $\tau_{\rm ac}$), our objective is the analysis of the noise spectra in the presence of GR and ac fields, and the main conclusions of our work can be extended to the case when these processes take place at lower frequencies.

III. NOISE CALCULATION

The fluctuations will be studied through the calculation of the spectral density of current fluctuations $S_I(f)$, defined as

$$S_I(f)=2\int_{-\infty}^{\infty} C_I(t)\exp(i\omega t)dt=4\int_0^{\infty} C_I(t)\cos(\omega t)dt, \tag{4}$$

where $C_I(t)=\langle \delta I(0)\,\delta I(t)\rangle$ is the autocorrelation function of current fluctuations $\delta I(t)=I(t)-\langle I\rangle$, the angular brackets indicating time average, and $\omega=2\pi f$. According to Eq. (3), the current can be written as[11]

$$I(t)=\frac{q}{L}N_f(t)v(t), \tag{5}$$

where $v(t)=[1/N_f(t)]\Sigma_{i=1}^{N_f(t)}v_{xi}(t)$ is the mean velocity of the free carriers at time t. Equation (5) allows the decomposition of $C_I(t)$ into three main contributions $C_I(t)=C_V(t)+C_N(t)+C_{VN}(t)$ [and therefore $S_I(f)=S_V(f)+S_N(f)+S_{VN}(f)$] associated, respectively, with the fluctuations of the mean velocity of electrons [$\delta v(t)=v(t)-\langle v\rangle$, thermal noise] C_V, the fluctuations of the free-carrier number [$\delta N_f(t)=N_f(t)-\langle N_f\rangle$, GR noise] C_N, and their cross correlation C_{VN}. The corresponding formulas are given by[11,25]

$$C_V(t)=\frac{q^2}{L^2}\langle N_f\rangle^2\langle \delta v(0)\,\delta v(t)\rangle=\frac{q^2}{L^2}\langle N_f\rangle^2 C_v(t), \tag{6}$$

$$C_N(t)=\frac{q^2}{L^2}\langle v\rangle^2\langle \delta N_f(0)\,\delta N_f(t)\rangle=\frac{q^2}{L^2}\langle v\rangle^2 C_n(t), \tag{7}$$

$$C_{VN}(t)=\frac{q^2}{L^2}\langle v\rangle\langle N_f\rangle\langle \delta v(0)\,\delta N_f(t)+\delta N_f(0)\,\delta v(t)\rangle$$

$$=\frac{q^2}{L^2}\langle v\rangle\langle N_f\rangle C_{vn}. \tag{8}$$

In this way, the contributions associated with the different sources of fluctuations responsible for the noise spectrum at a given field are clearly individuated and accounted for within the same microscopic level. $\langle v\rangle$, $\langle N_f\rangle$, $C_v(t)$, $C_n(t)$, and $C_{vn}(t)$ are evaluated from the sequence of $v(t)$ and $N_f(t)$ obtained from the MC simulation.

According to the microscopic model used in the simulation, it is expected that $S_v(f)$ and $S_n(f)$ [Fourier transforms of $C_v(t)$ and $C_n(t)$] exhibit Lorentzian shapes;

$$S_v(f)=\frac{4\langle \delta\nu^2\rangle\tau_f}{1+\omega^2\tau_f^2}, \tag{9}$$

$$S_n(f)=\frac{4\langle \delta N_f^2\rangle\tau_1}{1+\omega^2\tau_1^2}, \tag{10}$$

where $\tau_l=\tau_g\tau_r/(\tau_g+\tau_r)$ is the carrier lifetime, $\langle \delta N_f^2\rangle=N\tau_r\tau_g/(\tau_r+\tau_g)^2$ and $\langle \delta v^2\rangle=kT/(m\langle N_f\rangle)$ (as long as the carriers remain close to equilibrium conditions) with $\langle N_f\rangle=N\tau_r/(\tau_r+\tau_g)$.[3] All these predictions will be checked with the simulations of the semiconductor under the action of dc fields.

When a time-varying field of the type $E(t)=E_{\rm ac}\sin(2\pi f_{\rm ac}t)$ is applied to the semiconductor, according to our linear model a deterministic time-dependent linear response in the current $I_d(t)$ is expected: $I_d(t)=(q/L)\times\langle N_f\rangle v_d(t)$, where $v_d(t)=\mu E(t)$, $\mu=q\tau_f/m$ being the carrier mobility. In fact, by defining $\delta v'(t)=v(t)-v_d(t)$ as the fluctuation of velocity over the average deterministic value, the instantaneous current can be written as

$$I(t)=\frac{q}{L}[\langle N_f\rangle v_d(t)+\langle N_f\rangle\delta v'(t)+v_d(t)\,\delta N_f(t)$$

$$+\delta N_f(t)\,\delta v'(t)]. \tag{11}$$

Due to the number fluctuations originated by the trapping–detrapping processes, a term of the form $(q/L)v_d(t)\,\delta N_f(t)$ appears in $I(t)$, which corresponds to an amplitude modulation of the current response by number fluctuations. This term should lead to the upconversion of the low-frequency GR spectrum, contributing with sidebands centered around $f_{\rm ac}$. The main objective of our work is the detection and the

analysis of this effect. Due to the very large difference existing between the amplitude of the deterministic response of the sample and that of the unconverted GR contribution, both appearing at (or around) f_{ac}, we will analyze the current fluctuations over the deterministic component, $\delta I_{ac}(t)=I(t)-I_d(t)$, thus eliminating from the spectrum the peak at f_{ac} associated to $I_d(t)$, which would make difficult the detection of the GR contribution around f_{ac}. A similar procedure is necessary in experimental measurements.[8–10]

From Eq. (11), a decomposition of $C_I^{ac}(t)=\langle \delta I_{ac}(0)\,\delta I_{ac}(t)\rangle$ into velocity C_V^{ac}, number C_N^{ac} and cross-correlation C_{VN}^{ac} contributions can also be performed as

$$C_V^{ac}(t)=\frac{q^2}{L^2}\langle N_f\rangle^2\langle \delta v'(0)\,\delta v'(t)\rangle, \tag{12}$$

$$C_N^{ac}(t)=\frac{q^2}{L^2}\langle v_d(0)\,\delta N_f(0) v_d(t)\,\delta N_f(t)\rangle, \tag{13}$$

$$C_{VN}^{ac}(t)=\frac{q^2}{L^2}\langle N_f\rangle\langle \delta v'(0) v_d(t)\,\delta N_f(t) + v_d(0)\,\delta N_f(0)\,\delta v'(t)\rangle, \tag{14}$$

where second order terms in fluctuations have been neglected. These expressions will be used only in some specific cases to identify the origin of the different contributions to the noise spectra. In most cases, in order to obtain more reliable results and save computer time, we will evaluate the spectral density of current fluctuations directly by squaring the Fourier transform of $\delta I_{ac}(t)$.[3,26]

Finally we would like to stress that most of the assumptions of our model (energy-independent scattering and trapping probabilities, thermalizing scattering) are made with the aim of achieving a linear response of the semiconductor sample to time-varying fields, thus avoiding the generation of harmonics which would reduce considerably the efficiency of the upconversion process that we want to analyze.

IV. RESULTS

A. dc electric field

In this section we show some significant results concerning the time and frequency behavior of current noise in the semiconductor sample under analysis when a steady electric field is applied. These results will illustrate the main features of thermal and GR noise present in the structure.

Figure 1(a) shows the autocorrelation functions of velocity and number fluctuations, $C_v(t)$ and $C_n(t)$, respectively, for the case of equilibrium conditions ($E=0$) and $\tau_r=2$ ps, $\tau_g=18$ ps. Both autocorrelation functions show the expected exponential behavior with relaxation times given by $\tau_f\cong\tau_s=0.01$ ps for $C_v(t)$ and $\tau_l=1.8$ ps for $C_n(t)$, with the zero-time values in close agreement with theoretical predictions: $\langle \delta v^2\rangle=kT/(m\langle N_f\rangle)=1.82\times10^8\ \mathrm{m^2/s^2}$ and $\langle \delta N_f^2\rangle=N\tau_r\tau_g/(\tau_r+\tau_g)^2=90$. In Fig. 1(b) the corresponding spectral densities are reported. They exhibit the expected Lorentzian shape with cutoff frequencies associated with the corresponding relaxation times, which differ by more than two orders of magnitude. The excellent agreement of these spectra with the theoretical predictions given by Eqs. (9) and (10) validate the model and simulation scheme used in the calculations. Within the present model for scattering and trapping mechanisms, with energy-independent probabilities, there is no physical process correlating number and velocity fluctuations. Consequently, the cross terms $C_{vn}(t)$ and $S_{vn}(f)$ are always found to be negligible in the calculations.

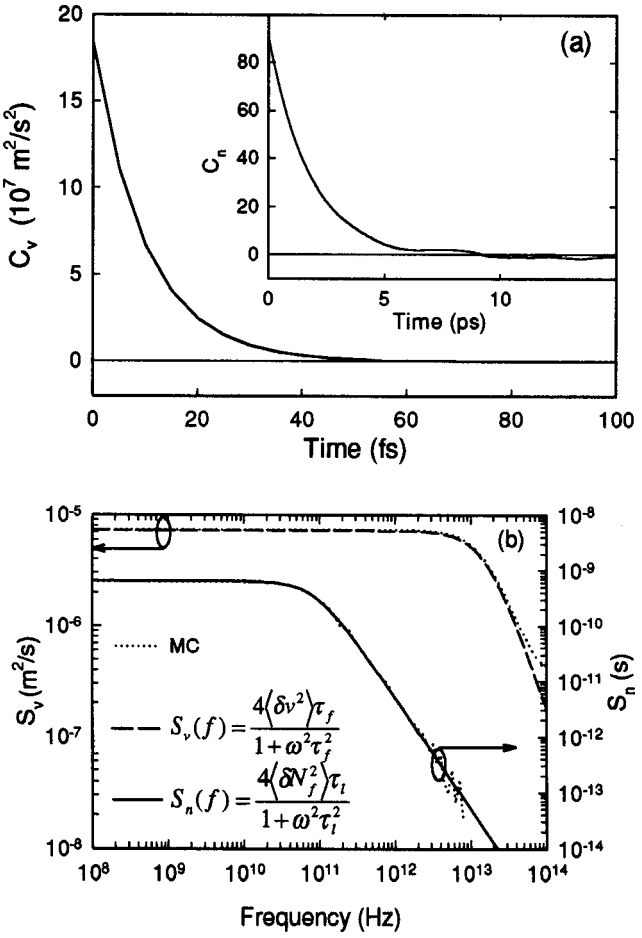

FIG. 1. (a) Autocorrelation functions of velocity and number fluctuations (inset) at equilibrium for $\tau_r=2$ ps, $\tau_g=18$ ps; (b) corresponding spectral densities together with theoretical predictions [Eqs. (9) and (10)].

The contributions of number and velocity fluctuations to the noise in the current under far-from-equilibrium conditions ($E=50$ kV/cm) for the same characteristic times of the previous figure are shown in Fig. 2. $C_I(t)$ shows a short-time decay associated with the velocity contribution $C_V(t)$, and a further slow decay related to the number contribution $C_N(t)$. The corresponding current-noise spectrum $S_I(f)$ is just the superposition of two Lorentzians, $S_V(f)$ and $S_N(f)$, with cutoff frequencies determined by τ_f and τ_l, respectively. Thus, $S_I(f)$ exhibits two plateaus: a first one at low frequency due to GR noise, and a second one related to thermal noise in the range between the two cutoff frequencies. According to Eqs. (6) and (7), for a given set of characteristic times (τ_s, τ_r, and τ_g), the amplitude of the former plateau is proportional to $\langle I\rangle^2$, while that of the latter is proportional to $\langle N_f\rangle$ and also to the electronic temperature (in our model always close to the lattice temperature except for very high electric fields). This is better illustrated in Fig. 3.

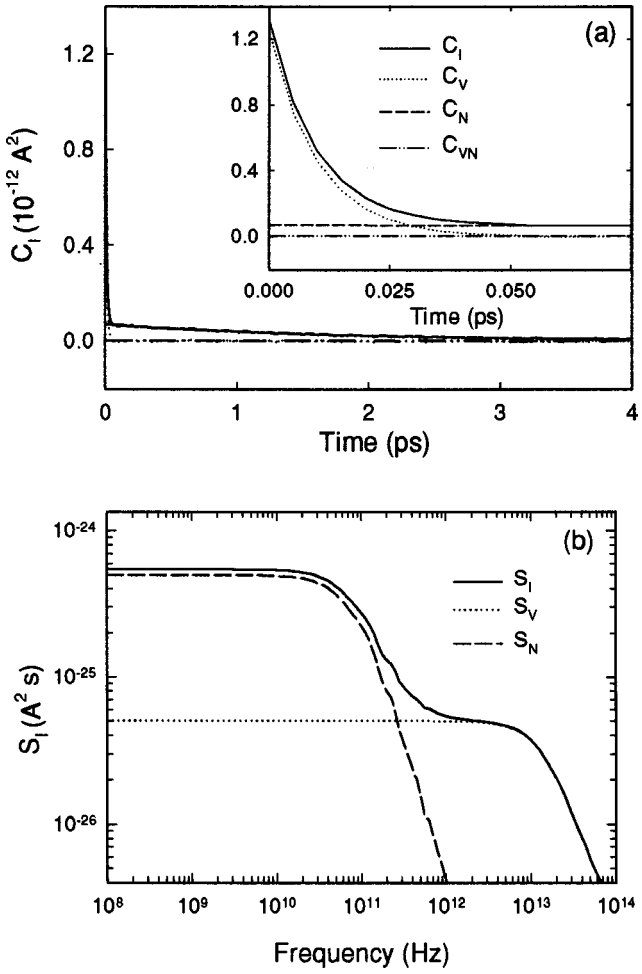

FIG. 2. (a) Autocorrelation function of current fluctuations and decomposition into the contributions associated with velocity and number fluctuations for an electric field of 50 kV/cm and $\tau_r=2$ ps, $\tau_g=18$ ps. The inset details the short-time behavior, (b) corresponding spectral densities.

The evolution of $S_I(f)$ with increasing values of E is reported in Fig. 3. The characteristic times are the same as in previous figures and equal for the different fields; therefore $\langle N_f\rangle = N\tau_r/(\tau_r+\tau_g)=100$ is also the same. In the case of equilibrium conditions, only velocity fluctuations contribute to the current noise. GR noise (though also present at equilibrium as observed in Fig. 1), being a source of excess noise, only contributes to the noise at the terminals in the presence of a net current flowing through the structure [see Eq. (7)]. This is observed for increasing values of E, for which the contribution of $S_N(f)$ (low-frequency plateau) increases with the field. Remarkably, despite the fact that $\langle N_f\rangle$ is the same for several fields, a significant increase is observed in the plateau related to thermal noise, especially for 100 kV/cm. For low fields, carriers are close to equilibrium, and $\langle \delta v^2\rangle \cong kT/(m\langle N_f\rangle)$. However, at sufficiently high fields inelastic scattering is no longer able to dissipate all the energy gained by the carriers from the field (hot-electron regime).[19] In such a case $\langle \delta v^2\rangle$ would be better estimated by using the concept of electron temperature $T_e > T$ as $\langle \delta v^2\rangle = kT_e/(m\langle N_f\rangle)$, thus leading to the increase of the thermal noise plateau.

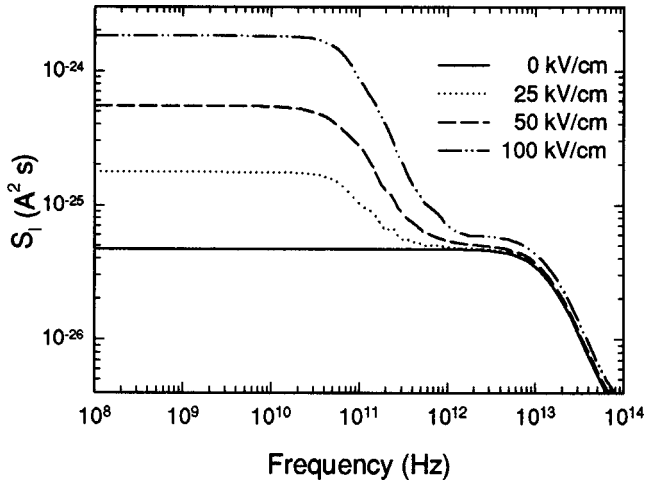

FIG. 3. Current spectral density for different values of the electric field and $\tau_r=2$ ps, $\tau_g=18$ ps.

To investigate the influence of τ_r and τ_g on the noise, we explore some possible choices for the values of these times, thus modifying the lifetime τ_l and the average free-carrier number $\langle N_f\rangle$. For the same field of 50 kV/cm, in Fig. 4 we analyze three different sets of values: (a) $\tau_r=5.5$ ps, $\tau_g=145.8$ ps ($\tau_l=5.3$ ps, $\langle N_f\rangle=36.35$); (b) $\tau_r=2$ ps, $\tau_g=18$ ps ($\tau_l=1.8$ ps, $\langle N_f\rangle=100$); (c) $\tau_r=2$ ps, $\tau_g=2$ ps, ($\tau_l=1$ ps, $\langle N_f\rangle=500$). The sets (a) and (b) lead to a similar value of the GR noise plateau, while set (c) provides a higher value [see Eq. (10)]. The cutoff frequency of GR noise becomes higher as τ_l decreases, thus being lower for case (a) and then increasing for cases (b) and (c). The influence of the different value of $\langle N_f\rangle$ in each case is clearly observed in the level of thermal noise. Since $\tau_r \gg \tau_s$, then $\tau_f \cong \tau_s$ in the three cases (and $\langle v\rangle$ takes the same value); consequently, the cutoff frequency of thermal noise is practically the same for the three sets of times.

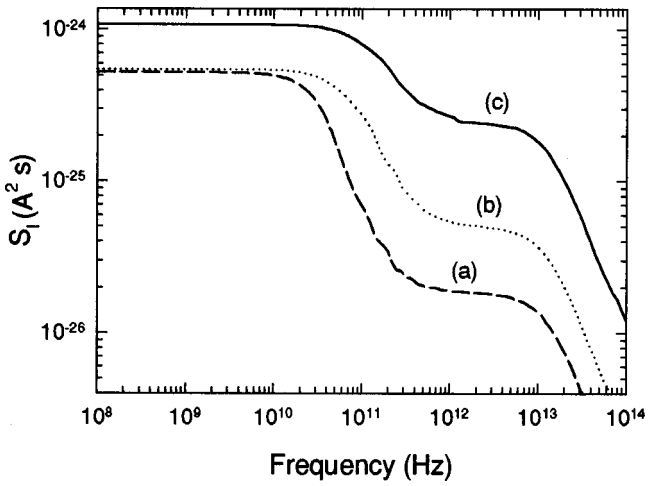

FIG. 4. Current spectral density for an electric field of 50 kV/cm and different sets of times: (a) $\tau_r=5.5$ ps, $\tau_g=145.8$ ps; (b) $\tau_r=2$ ps, $\tau_g=18$ ps; (c) $\tau_r=2$ ps, $\tau_g=2$ ps.

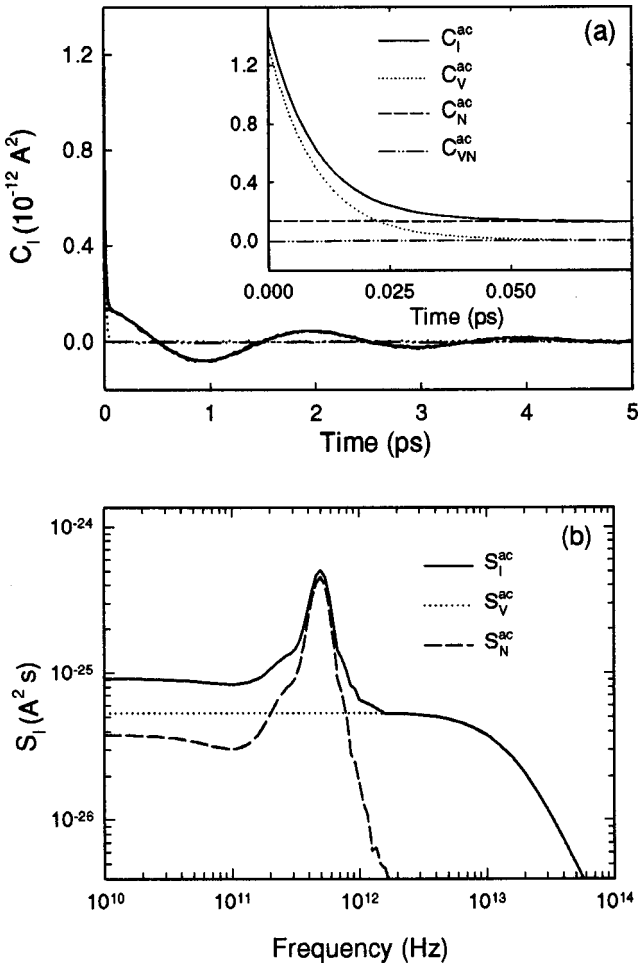

FIG. 5. (a) Autocorrelation function of current fluctuations and decomposition into the contributions associated with velocity and number fluctuations for a time-varying electric field of amplitude 100 kV/cm and $\tau_r=2$ ps, $\tau_g=18$ ps. The inset details the short-time behavior; (b) corresponding spectral densities.

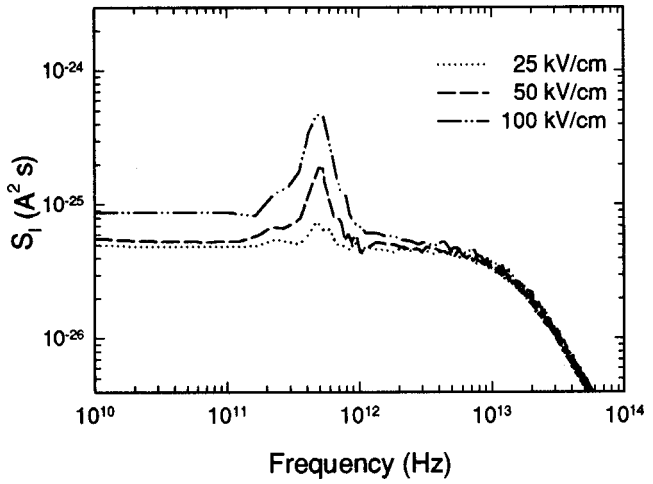

FIG. 6. Current spectral density for different values of the time-varying electric field amplitude and $\tau_r=2$ ps, $\tau_g=18$ ps.

B. Time-varying electric field

After the presentation of dc electric fields, we focus on the discussion of the main features observed when a time-varying electric field $E(t)=E_{ac}\sin(2\pi f_{ac}t)$ is applied to the structure (and in the absence of dc field). Due to the requirement of a reasonable CPU time and the large difference in the time scales involved in the problem, we have chosen a very high frequency of 500 GHz for $E(t)$. Nevertheless, the results obtained here can be readily extended to lower frequencies, as rf and microwaves. In order to compare the ac with the previous dc results we will report the current spectral density for physical conditions already considered in the previous section. On the other hand, most of the results shown here are obtained by performing directly the Fourier transform of the current, and then squaring it.[26] For this reason the spectral densities reported in this section are somewhat ''noisier'' than those of the previous section. With this technique we avoid the calculation of extremely long correlation functions which can be evaluated only in some cases (short τ_I) and may provide less reliable results.

A case in which the calculation of the correlation functions is affordable is shown in Fig. 5, corresponding to $E_{ac}=100$ kV/cm and $\tau_r=2$ ps, $\tau_g=18$ ps. Here, the origin of the different contributions to the noise spectrum can be clearly identified. $C_V^{ac}(t)$ remains practically identical to $C_V(t)$ obtained under dc fields. The main novelty in the results comes from $C_N^{ac}(t)$, which shows a damped oscillatory behavior at the frequency of the electric field, thus leading to the appearance of a significant noise contribution around f_{ac} in the spectrum, in addition to that of thermal noise. The origin of this contribution is the amplitude modulation of the semiconductor ac response associated with the fluctuation of the carrier number originated by GR phenomena. As in the dc case, $C_{VN}^{ac}(t)$ is also found to be negligible. The carrier number fluctuations presently evidenced would lead to fluctuations of the sample conductance independent of the applied voltage. This fluctuating conductance would appear as a linear time-varying (LTV) element, also defined as a ''parametric conductance,'' in circuit theory.[27]

$S_I(f)$ as a function of frequency for different values of E_{ac} is shown in Fig. 6 for $\tau_r=2$ ps and $\tau_g=18$ ps (same characteristic times used in Fig. 3). A significant peak around f_{ac} (500 GHz) is observed in the spectra (whose amplitude increases with E_{ac}), which is associated with the upconversion of the low-frequency noise. The low-frequency GR noise spectrum appears transferred to high frequency as two sidebands around the oscillation frequency of the electric field. Though difficult to appreciate in the figure, the bandwidth of the noise detected around f_{ac} corresponds precisely to that of the low-frequency GR noise. This occurs with the amplitude of the upconverted spectrum. As observed, the level of thermal noise is practically the same as that obtained in the static case, as expected when an energy-independent τ_s is considered.

Remarkably, these results indicate the emergence (and possibility of detection) of GR noise (an excess noise source) even in the absence of a dc current flowing through the semiconductor (no dc field is applied). Some authors based this idea on measurements of GR noise at high frequencies.[8,9] In order to detect it clearly, two main considerations must be taken into account (both experimentally and numerically). The first one is relative to the ratio between the frequency of

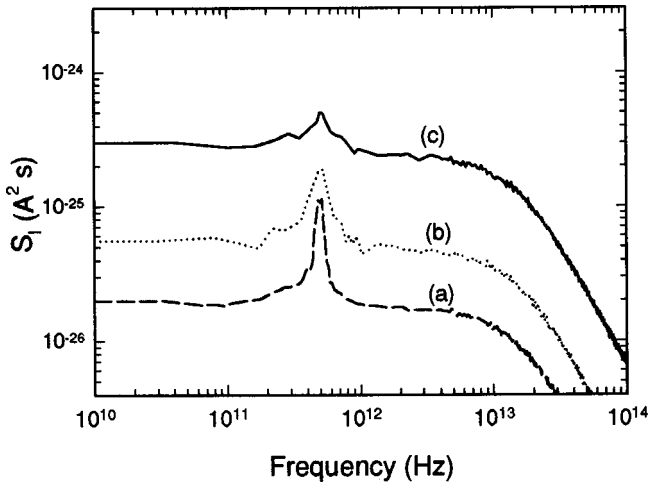

FIG. 7. Current spectral density for a time-varying electric field of amplitude 50 kV/cm and different sets of times: (a) $\tau_r = 5.5$ ps, $\tau_g = 145.8$ ps; (b) $\tau_r = 2$ ps, $\tau_g = 18$ ps; (c) $\tau_r = 2$ ps, $\tau_g = 2$ ps.

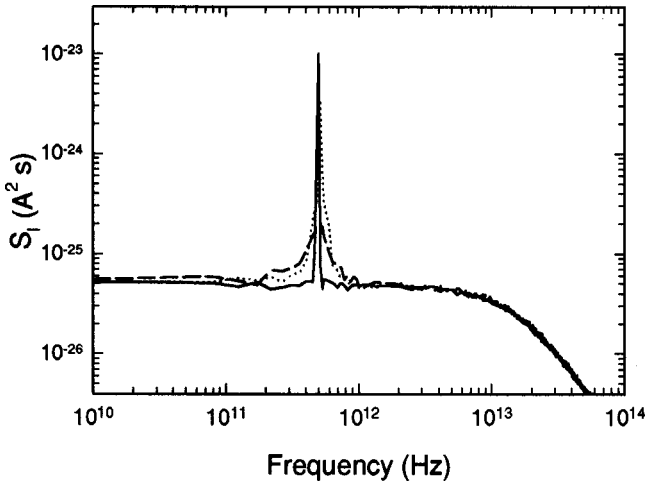

FIG. 8. Current spectral density for a time-varying electric field of amplitude 50 kV/cm and different sets of times leading to the same number of free carriers (100). Solid line corresponds to $\tau_r = 200$ ps, $\tau_g = 1800$ ps; dotted line to $\tau_r = 20$ ps, $\tau_g = 180$ ps; and dashed line to $\tau_r = 2$ ps, $\tau_g = 18$ ps.

the electric field and the bandwidth of noise: small noise bandwidths apparently disappear with extremely high f_{ac}. Second, according to our calculations there is a very large difference in the amplitude of the upconverted sidebands and the semiconductor response at the ac frequency (typically several orders of magnitude), which makes the detection of the GR contribution very difficult. To this end, it is necessary to suppress from the output current the frequency of the time-varying signal,[9] as done in our calculations by removing the deterministic component of the current.

Figure 6 indicates that under ac fields GR noise may also have some influence at low frequency if the GR noise cutoff and the ac frequency are not far enough. In fact, $S_I(0)$ can be higher than the expected thermal noise due to the large extension of the lower sideband, reaching the zero-frequency value. This explains, for example, the different values that $S_I(f)$ takes in Fig. 6 for low and high frequency (in the thermal noise plateau), especially for $E_{ac} = 100$ kV/cm; also observed in Fig. 5(b).

Figure 7 shows the influence of τ_r and τ_g on the noise under dynamic conditions for the same field magnitude and sets of characteristic times as those used in Fig. 4. In contrast with static conditions, where cases (a) and (b) showed a similar low-frequency value, here every curve is clearly distinguishable from each other. As observed, case (a) corresponds to the smallest bandwidth of GR noise, and due to the big difference between the levels of thermal and upconverted GR noise (see Fig. 4), the peak around f_{ac} is particularly pronounced. The sidebands around f_{ac} can be clearly noticed in case (b), with wider bandwidth than case (a). Finally, in case (c) a high value of upconverted GR noise is obtained, but it is difficult to distinguish it from thermal noise because both levels of noise are similar (see Fig. 4). The largest bandwidth corresponds to case (c), which is reflected in the fact that the lower sideband extends up to low frequency, leading to a noise level significantly higher than that of the high-frequency thermal noise plateau.

Thermal noise has an indirect dependence on the GR rates, since it is proportional to $\langle N_f \rangle$. This can be observed in Fig. 8 where the current spectral densities for $E_{ac} = 50$ kV/cm and $\tau_r = 200$ ps, $\tau_g = 1800$ ps (solid line); $\tau_r = 20$ ps, $\tau_g = 180$ ps (dotted line); and $\tau_r = 2$ ps, $\tau_g = 18$ ps (dashed line) are depicted; the three sets of times leading to the same average number of free carriers $\langle N_f \rangle = 100$, and therefore to the same level of thermal noise. However the upconverted GR spectra shows a different shape related to the values of the trapping–detrapping characteristic times. Thus, the bandwidth increases when the lifetime of carriers decreases. In fact, if the bandwidth of GR noise is narrow as compared with the frequency of the electric field (case of solid line), it can be very difficult to be detected (or measured) when the total current spectral density is evaluated without removing the deterministic component, and in the worst case the effect of GR noise can be incorrectly neglected. On the other hand, higher values of the peak are obtained when τ_l increases, according to Eq. (10).

We have not shown results for the case when the electric field also contains a dc component, since in such a case there is no new effect. Simply, in the presence of a dc current, in addition to the upconversion, the GR spectrum is evidenced at low frequency with the features reported in the previous section. Eventually, and depending on the bandwidth of GR noise, an overlap of the low-frequency GR plateau with the lower upconverted sideband can take place.

V. CONCLUSIONS

An ensemble MC simulation has been used to investigate the noise spectra of a semiconductor sample in the presence of scattering mechanisms and GR processes under both dc and ac electric fields. This method, by incorporating the processes at the origin of the fluctuations, allows for a direct microscopic interpretation of the noise spectra. We have used a simple model where the characteristic times of the different physical processes are energy independent to ensure the linearity in the response of the system, thus making possible the identification of the contributions of the different

noise sources to the current spectra under time-varying fields, when the upconversion of the low-frequency GR noise takes place.

The current spectral densities calculated under static electric field are in close agreement with theoretical predictions, thus confirming the validity of the model and MC simulation. GR noise is found to increase with the current and shows a cutoff frequency related to the carrier lifetime. The level of thermal noise depends on the number of free carriers and on the scattering time (as long as this time is shorter than the recombination time), which also determines the cutoff at high frequencies. For high electric fields, when inelastic scattering is no longer able to dissipate the energy gained by the carriers in the free flights, electrons become hot and the thermal noise plateau is found to increase due to the higher electron temperature.

The MC results evidence that the amplitude modulation of the semiconductor current response to a time-varying electric field due to GR phenomena leads to the upconversion of the low-frequency GR noise spectrum, which appears as sidebands around the frequency of the ac signal. Remarkably, though GR noise is an excess noise source, this effect takes place even in the absence of dc current. In order to detect this phenomenon, it was necessary to remove from the current the deterministic linear response of the sample. The width and amplitude of the low-frequency GR spectra have been checked to be in agreement with those of the corresponding sidebands appearing around the frequency of the ac signal, thus confirming the upconversion of GR noise. Within our model, the level of thermal noise is found to remain unaltered under dynamic conditions. Note that $1/f$ fluctuations of the low-field mobility appear as a LTV conductance, it may be conjectured that the results obtained here for carrier number fluctuations may be extended to this fundamental $1/f$ noise.

Finally, we remark that in this work we assumed a simple model leading to a semiconductor linear response to clearly evidence the GR noise upconversion. The analysis of similar processes in real semiconductors where nonlinear effects can take place (energy dependence of characteristic times, velocity saturation, coupling among different fluctuations, harmonic generation in the ac response, etc.) and their influence in semiconductor devices is the objective of our forthcoming work.

ACKNOWLEDGMENTS

The authors gratefully acknowledge helpful discussions with Professor D. Pardo and Dr. J. Mateos. This work has been partially supported by Project Nos. PB97-1331 from the Dirección General de Enseñanza Superior e Investigación Científica and SA44/99 from the Consejería de Educación y Cultura de la Junta de Castilla y León.

[1] J. A. Copeland, IEEE Trans. Electron Devices **ED-18**, 50 (1971).
[2] L. D. Yau and C. T. Sah, IEEE Trans. Electron Devices **ED-16**, 160 (1969).
[3] A. Van der Ziel, *Noise in Solid State Devices and Circuits* (Wiley, New York, 1986).
[4] D. Rigaud and M. Valenza, IEEE Trans. Electron Devices **41**, 2076 (1994).
[5] P. O. Lauritzen, Solid-State Electron. **8**, 41 (1965).
[6] M. N. Tutt, D. Pavlidis, A. Khatizadeh, and B. Bayraktaroglu, IEEE Trans. Microwave Theory Tech. **43**, 1461 (1995).
[7] H. Darabi and A. A. Abidi, IEEE J. Solid-State Circuits **33**, 15 (2000).
[8] J. Obregon, M. Prigent, J. C. Nallatamby, M. Camiade, D. Rigaud, and R. Quere, Workshop on Microwave Oscillators: 2000 IEEE MTT-S International Microwave Symposium, Boston, 2000 (to be published).
[9] J. H. Lorteije and A. M. H. Hoppenbrowers, Philips Res. Rep. **26**, 29 (1971).
[10] F. N. Hooge, T. G. M. Kleinpenning, and L. K. J. Vandamme, Rep. Prog. Phys. **44**, 31 (1981).
[11] L. Varani, L. Reggiani, T. Kuhn, T. González, and D. Pardo, IEEE Trans. Electron Devices **41**, 1916 (1994).
[12] G. Hill, P. N. Robson, and W. Fawcett, J. Appl. Phys. **50**, 356 (1979).
[13] R. Fauquembergue, J. Zimmermann, A. Kaszynski, E. Constant, and J. P. Nougier, J. Appl. Phys. **51**, 1065 (1980).
[14] J. G. Adams, T.-W. Tang, and L. E. Kay, IEEE Trans. Electron Devices **41**, 575 (1994).
[15] T. González, D. Pardo, L. Varani, and L. Reggiani, IEEE Trans. Electron Devices **42**, 991 (1995).
[16] M. J. Martín, D. Pardo, and J. E. Velázquez, J. Appl. Phys. **84**, 5012 (1998).
[17] T. González, D. Pardo, L. Reggiani, and L. Varani, J. Appl. Phys. **82**, 2349 (1997).
[18] J. Mateos, T. González, D. Pardo, V. Hoel, and A. Cappy, Semicond. Sci. Technol. **14**, 864 (1999).
[19] M. Macucci, B. Pellegrini, P. Terreni, and L. Reggiani, J. Appl. Phys. **63**, 5369 (1988).
[20] T. Kuhn, L. Reggiani, L. Varani, and V. Mitin, Phys. Rev. B **42**, 5702 (1990).
[21] T. Kuhn, L. Reggiani, and L. Varani, Phys. Rev. B **42**, 11133 (1990).
[22] T. Kuhn, L. Reggiani, L. Varani, D. Gasquet, J. C. Vaissiere, and J. P. Nougier, Phys. Rev. B **44**, 1074 (1991).
[23] C. Jacoboni and P. Lugli, *The Monte Carlo Method for Semiconductor Device Simulation* (Springer, Berlin, 1989).
[24] A. van der Ziel, *Solid State Physical Electronics* (Prentice-Hall, Englewood Cliffs, NJ, 1976).
[25] L. Reggiani, T. Kuhn, and L. Varani, Appl. Phys. A: Solids Surf. **54**, 411 (1992).
[26] W. H. Press, B. P. Flannery, S. A. Teukolsky, and W. T. Vetterling, *Numerical Recipes* (Cambridge University Press, New York, 1992).
[27] F. Kornil and K. Urba, *Nonlinear and Parametric Circuits* (Wiley, Chichester, 1988).